Revista de la Academia Colombiana de Ciencias Exactas, Físicas y Naturales
49(193):818-832, octubre-diciembre de 2025. doi: https://doi.org/10.18257/raccefyn.3187

Original article

Biogenic synthesis of silver-functionalized iron and copper oxide nanocomposites using the aqueous extract of *Psidium guajava* fruit

Síntesis biogénica de nanocompuestos de óxidos de cobre y de hierro funcionalizados con plata utilizando el extracto acuoso del fruto de *Psidium guajava*

Michael Castañeda-Mendoza[1,*], Gabriel Leonardo Mora-Najar[1], Claudia Liliana Sánchez-Sáenz[3], Rolando Javier Rincón-Ortiz[2], Cristian Camilo Ramírez-Fosca[2], Indry Milena Saavedra-Gaona[1], Daniel Llamosa-Pérez[2], Carlos Arturo Parra-Vargas[1]

[1] Grupo de Física de Materiales, Escuela de Física, Universidad Pedagógica y Tecnológica de Colombia, Tunja, Colombia
[2] Grupo de Investigación Fundamental y Aplicada en Materiales, Universidad Antonio Nariño, Bogotá D.C., Colombia
[3] Grupo de Investigación en Telemática y TIC Aplicadas, Facultad de Ingeniería, Universidad Pedagógica y Tecnológica de Colombia, Tunja, Colombia

Abstract

Here, we present a green coprecipitation synthesis route for silver-functionalized copper and iron oxide nanocomposites (Cu_2O/CuO/Fe_2O_3@Ag) using guava (*Psidium guajava)* fruit extract as reducing and stabilizing agent. The novelty of this approach lies in the unexplored use of guava, a widely available biomass rich in phytochemicals, to produce multifunctional nanocomposites with enhanced properties. The structural and morphological analyses (XRD, FTIR, SEM, TEM) confirmed the presence of crystalline phases of Fe_2O_3, Cu_2O, CuO, and Ag, along with nanoflake-like and spheric-like morphologies and nanometric particle sizes. Magnetic characterization (VSM) revealed a change from paramagnetic behavior in non-functionalized samples to weak ferromagnetism with reduced coercivity and magnetization upon silver incorporation. The antibacterial assays demonstrated that the functionalized nanocomposites exhibited strong inhibitory effects against the multidrug-resistant pathogen *Klebsiella pneumoniae*, achieving substantial growth inhibition at 500 ppm. Our findings highlight the potential of guava fruit extract as a sustainable precursor for the biogenic synthesis of silver-functionalized Fe–Cu oxide nanocomposites, offering a promising route for environmentally friendly nanomaterials with applications in biomedical and environmental fields.

Keywords: Green chemistry; Nanomaterials; Copper oxide; Iron oxide; Guava fruit extract; Antibacterial.

Resumen

Presentamos aquí una ruta verde de síntesis por coprecipitación de nanocompuestos de oxidos de cobre y de hierro funcionalizados con plata (Cu_2O/CuO/Fe_2O_3@Ag) utilizando extracto de guayaba (*Psidium guajava)* como agente reductor y estabilizador. La novedad de este enfoque radica en el uso inexplorado de la guayaba, una biomasa rica en fitoquímicos ampliamente disponible, para producir nanocompuestos multifuncionales con propiedades mejoradas. Los análisis estructurales y morfológicos (XRD, FTIR, SEM, TEM) confirmaron la presencia de fases cristalinas de Fe_2O_3, Cu_2O, CuO y Ag, además de morfologías similares a nanoescamas y tamaños de partícula nanométricos. La caracterización magnética (VSM) reveló el cambio del comportamiento paramagnético en muestras no funcionalizadas a un ferromagnetismo débil con coercitividad y magnetización reducidas tras la incorporación de plata. Los ensayos antibacterianos demostraron que los nanocompuestos funcionalizados exhibían fuertes efectos inhibidores contra el patógeno resistente a múltiples

Citation: Castañeda-Mendoza M., *et al*. Biogenic synthesis of silver-functionalized iron and copper oxide nanocomposites using the aqueous extract of *Psidium guajava* fruit. Revista de la Academia Colombiana de Ciencias Exactas, Físicas y Naturales. 49(193):818-832, octubre-diciembre de 2025. doi: https://doi.org/10.18257/raccefyn.3187

Editor: Rafael Gonzalez

***Corresponding autor:**
Michael Castaneda-Mendoza;
michael.castaneda@uptc.edu.co - castanedamendozamichael@gmail.com

Received: March 25, 2025
Accepted: September 2, 2025
Published on line: October 15, 2025

fármacos *Klebsiella pneumoniae*, logrando una inhibición sustancial del crecimiento a 500 ppm. Estos hallazgos destacan el potencial del extracto de la guayaba como precursor sostenible para la síntesis biogénica de nanocompuestos de los óxidos de Fe y Cu funcionalizados con plata, lo que ofrece una ruta prometedora para la obtención de nanomateriales respetuosos del medio ambiente con aplicaciones en campos biomédicos y ambientales.

Palabras clave: Química verde; Nanomateriales: óxido de cobre; Óxido de hierro; Extracto de guayaba; Antibacteriano.

Introduction

Nanomaterials (NM) have gained significant attention in recent decades due to their wide range of applications, including environmental remediation (**Kumar *et al.***, 2022), renewable energies (**Akin *et al.***, 2019), biomedicine (**Naik *et al.***, 2023), and industries (**Paidari & Ibrahim**, 2021), among others. The vast spectrum of NM uses arises from the unique properties they exhibit; some of their most notable characteristics include a high surface area-volume ratio (**Altammar**, 2023), ferrimagnetism (**Zahn *et al.***, 2022), and ferromagnetic and superparamagnetic behaviors (**Rashid *et al.***, 2022). This type of material has also shown promising properties in diagnosing and treating diseases such as cancer (**Jose *et al.***, 2020), serving as contrast agents in magnetic resonance imaging, drug delivery (**El-Boubbou *et al.***, 2016), and bactericidal applications (**Yang *et al.***, 2021). In this context, researchers have studied the biological and bactericidal properties of copper oxide and iron oxide nanostructures (**Bhavyasree & Xavier**, 2020; **Jamzad & Bidkorpeh**, 2020; **Sharma *et al.***, 2020), finding that specific iron oxide nanostructures like hematite (Fe_2O_3) exhibit high antimicrobial activity against bacteria such as *Pseudomonas aeruginosa* (**Yoonus *et al.***, 2021). Copper oxide nanoparticles, such as Cu_2O and delafossite ($CuFeO_2$), have also demonstrated notable antibacterial properties against various Gram-positive bacteria strains (*Bacillus subtilis*, *B. cereus*, and *Staphylococcus aureus*) and Gram-negative strains (*Escherichia coli* and *Xanthomonas campestris*) (**Antonoglou *et al.***, 2019).

Although copper and iron nano-oxides have shown bactericidal properties, they can be optimized by functionalizing their surfaces (**Yoonus *et al.***, 2021) using elements with appreciable antimicrobial qualities. Several metallic nanoparticles (NPs) exhibit these properties. Silver nanoparticles (Ag-NPs), for example, show high toxicity against a variety of microorganisms (**Parvekar *et al.***, 2020; **Salem *et al.***, 2020). These results suggest that the potential synthesis of a nanocomposite system integrating copper and iron oxides, functionalized with silver, may enhance bacteriostatic and bactericidal properties compared to their non-functionalized counterparts (**Antonoglou *et al.***, 2019).

On the other hand, the biogenic approach in NM synthesis has gained great relevance. In this regard, plants have been an ideal and abundant source of biomass useful in the synthesis, since the phytochemicals present in plant extracts can act as reducing and stabilizing agents of inorganic metal ions in NPs synthesis (**Chokkareddy & Redhi**, 2018). Several studies account for the use of plants' essential oils, fruits, roots, flowers, leaves, and stems to obtain NM (**Fakhari *et al.***, 2019; **Jadoun *et al.***, 2021; **Marslin *et al.***, 2018; **Charbgoo *et al.***, 2017; **Arsiya *et al.***, 2017; **Narayanan *et al.***, 2021; **Reddy**, 2017; **Ismail**, 2020; **Ramola *et al.***, 2019; **Tamoradi & Mousavi**, 2020; **Cahyana *et al.***, 2021; **Aksu Demirezen *et al.***, 2019; **Jacob *et al.***, 2017; **Veisi *et al.***, 2021; **Buarki *et al.***, 2022). In this context, Boyacá is one of the Colombian departments with the highest agrobiodiversity and agricultural production, producing 26,000 tons of vegetables and 98,000 tons of fruits in 2009 (**Ayala**, 2017), which shows tremendous possibilities given the availability of biological substances that may be used in this synthesis route. The antioxidant properties of guava have been widely evidenced in various studies using DPPH free radical scavenging tests (**Manikandan & Anand**, 2015). Its extracts have also shown inhibitory properties against several bacteria, among them, *Listeria monocytogenes and S. aureus* (**Mahfuzul Hoque *et al.***, 2007). Ripe guava fruits are rich in tannins, polyphenols with antioxidant properties, triterpenes, flavonoids, essential oils, saponins, carotenoids, lectins, fatty acids, fiber, and vitamins. Besides its high

Revista de la Academia Colombiana de Ciencias Exactas, Físicas y Naturales
49(193):818-832, octubre-diciembre de 2025. doi: https://doi.org/10.18257/raccefyn.3187

concentrations of vitamin C, higher than those of citrus fruits such as oranges or lemons, it contains appreciable amounts of vitamins A, B1, B2, niacin (B3), and pantothenic acid (B5), as well as appreciable amounts of phosphorus, calcium, iron, potassium, and sodium (**Rodríguez Medina & Valdés-Infante Herrero**, 2016).

Various studies have also described the green synthesis of metallic nanoparticles and simple oxide systems using plant extracts, but few have focused on Ag and Au NP or metal oxide nanocomposites obtained through phytogenic routes with guava leaf extracts (**Johurul Islam *et al.***, 2023; **Nguyen *et al.***, 2023; **Patil & Rane**, 2020; **Santhoshkumar *et al.***, 2014; **Sougandhi & Ramanaiah**, 2020). To the best of our knowledge, *P. guajava* fruit extract has not been explored as a reducing and stabilizing agent in this specific nanocomposite. The high bioavailability of this biomass, coupled with its great diversity of phytochemicals with reducing properties, makes the guava fruit an ideal candidate for the biogenic synthesis of NPs. Here, we report a silver-functionalized copper oxide and iron oxide nanocomposites biogenic route synthesis using *P. guajava* aqueous fruit extract as a reducing and stabilizing agent. We used X-ray diffraction (XRD), vibrating sample magnetometry (VSM), scanning electron microscopy (SEM), transmission electron microscopy (TEM), and Fourier transform infrared spectroscopy (FTIR) techniques for the structural, magnetic, and morphological characterization of the materials. Finally, we evaluated the bactericidal properties of the materials against strains of *K. pneumoniae*, a Gram-negative microorganism implicated in nosocomial diseases highly resistant to various antimicrobials and antibiotics (**Effah *et al.***, 2020). The integration of green synthesis with comprehensive structural and magnetic characterization, together with antibacterial assessment against *K. pneumoniae*, highlights the novelty and application potential of our study, particularly in Colombia, where guava is widely available.

Experimental details

Materials

Ripe guava fruit (variety Palmira-ICA1 reported by **Otálora *et al.*,** 2022) was sourced from the primary wholesale market in Tunja, Boyacá, Colombia; 98% purity iron sulfate heptahydrate $FeSO_4*7H_2O$ (CAS No. 7782-63-0) was purchased from Supelco-Ensure; 98% purity copper sulfate pentahydrate $CuSO_4*5H_2O$ (CAS No. 7758-99-8) was purchased from Merck; 99.9% purity silver nitrate $AgNO_3$ (CAS No. 7761-88-8) was purchased from Loba Chemie, and sodium hydroxide NaOH (CAS No. 1310-73-2) from PanReac AppliChem. All reagents were analytical grade.

Guava fruit extract preparation

Guava fruit extract was prepared using the modified method reported by **Kumar *et al.*** (2017). The fruit was thoroughly washed, ground, and filtered on a wide pore mesh; 10 g of the pulp obtained was taken and heated at 50°C in 50 mL of distilled water for 60 min under constant stirring at 1000 rpm and cooled at room temperature. The translucent, pink-colored extract was filtered with Whatman No. 1 filter paper, and then an extract/NaOH solution was prepared by dissolving 25.5 g of guava pulp in 60 mL of distilled water. Once the extract was obtained, 0.5 g of NaOH was added and completely dissolved.

Preparation of nanocomposites

The samples were obtained using the modified method reported by **Bhushan *et al.*** (2019). A stoichiometric amount of $CuSO_4*5H_2O$ was dissolved in 50 mL of distilled water at 50 °C. Then, 50 mL of a $FeSO_4*7H_2O$ solution was added to reach a Cu^{2+}:Fe^{2+} 1:1 molar ratio and, subsequently, 10 mL of the guava extract was added under constant stirring (1000 rpm) for 1 h. The pH was adjusted to 12, drop by drop, through the addition of a 0.2 M NaOH solution. Finally, the sample was aged at 50°C for 24 h to allow the NPS precipitation. The mixture was centrifuged and washed thrice at 2500 rpm for 20 min, then dried at 80 °C for 12 h. This procedure was repeated without the extract to obtain two systems: with extract (FeCu-G) and without it (FeCu).

Silver functionalization

Nanocomposite functionalization was done using the modified method reported by **Kooti *et al.*** (2013). Initially, 0.7 g of the material was dispersed in 50 mL of 0.05/0.202 (M) $AgNO_3$/Urea solution at room temperature and constant stirring (500 rpm) for 30 min to ensure the adsorption of Ag on the NPs, then, 10 mL of extract/NaOH solution was added to act as a stabilizing agent. After 5 minutes of reaction, 4 mL of guava extract was added as a reducing agent. The mixture obtained was heated to 70°C for 1 h to accelerate the reduction reaction. The functionalized nanocomposite was washed and centrifuged with distilled water at 3500 rpm for 20 min to remove any excess protective agents and alkaline materials, resulting in two samples: FeCuAg5 (without extract) and FeCuAg5-G (with extract). The $AgNO_3$/Urea ratio changed to 0.10/0.404 (M), obtaining the FeCuAg10 and FeCuAg10-G samples.

Characterization

The analysis was done in a Nicolet iS50 FTIR equipment using the attenuated total reflectance or ATR technique, recorded with a ZnSe crystal. The infrared spectra were collected in the wavenumber range from 2000 cm^{-1} to 500 cm^{-1}. For the crystalline structure analysis by XRD, we used an Empyrean diffractometer, with Cu-Kα radiation (λ=1.5406 Å) between 10° and 90°, a step width of 0.053°, a scanning speed of 2θ equals 2° per minute, and a measurement temperature of 293 K. For the TEM study, we used a LEO 440i scanning electron microscope, coating the samples with a thin Au-Pd layer, for the SEM analysis, a CARL ZEISS EVO MA 1 microscope, and to measure the fundamental magnetic properties of the synthesized materials, a Quantum Design Versalab magnetometer. Field-dependent magnetization measurements were taken from -30 to 30 kOe at room temperature (300 K). For temperature-dependent magnetization measurements, we used the Zero Field Cooled-Field Cooled (ZFC-FC) model varying the temperature in the 50 K- 400 K range at an applied field of 50 Oe. We evaluated the inhibition of bacterial growth by the nanocomposites using the microdilution technique in broth. We prepared and diluted 1 mg/mL (1000 ppm) solutions of each synthesized sample in microplates with the bacterial *K. pneumoniae* strain culture broths, starting from 30 ppm. Sodium hypochlorite (NaClO) at 7% was used as a control. The microplates were analyzed at 620 nm using an FC Multiskan TM plate reader.

Results and discussion

Structural characterization

Figure 1A shows the infrared spectra corresponding to the FeCu and FeCu-G samples. The characteristic CuO bands were observed at shorter wavenumber, around 580 cm^{-1}, indicating the vibrational modes of the bond between Cu-O atoms. Additionally, we observed the Cu–O stretching vibration bands around 1360 cm^{-1} (**Buledi *et al.***, 2021; **Sharmila *et al.***, 2018). This broadband from 500 to 900 cm^{-1} and the individual sharp peaks at 830 cm^{-1} were generally attributed to the metal-oxygen bond, indicating the Fe-O and Cu-O stretching vibration mode (**Jansanthea *et al.***, 2024; **Khalil *et al.***, 2017; **Nope *et al.***, 2025). The peak around 670 cm^{-1} responds to the Cu(I)-O bond (**Al-Senani *et al.***, 2022; **Castañeda-Mendoza *et al.***, 2025), their drastic decrease indicating a compositional change involving Cu_2O. A subsequent XRD analysis confirmed this transformation. The band around 1630 cm^{-1} was associated with the vibrational modes of the O–H bond bending due to the superficial water adsorption (**Amin *et al.***, 2016; **Apte *et al.***, 2007). In **Figure 1B**, the new band around 1550 cm^{-1} is usually attributed to the N-H bond vibrational modes and is common in these biogenic routes (**Sivaraj *et al.***, 2014). Furthermore, the use of urea in the functionalization process can explain the presence of this functional group. In general terms, the detection of fine spectral peaks between 577 cm^{-1} and 1030 cm^{-1}, with differentiated absorption bands for copper and iron oxides, corroborated the presence of these oxides in the samples, where the differences between the IR spectra of the functionalized and non-functionalized samples were attributed to the nanocomposites coating by Ag NPs.

Revista de la Academia Colombiana de Ciencias Exactas, Físicas y Naturales
49(193):818-832, octubre-diciembre de 2025. doi: https://doi.org/10.18257/raccefyn.3187

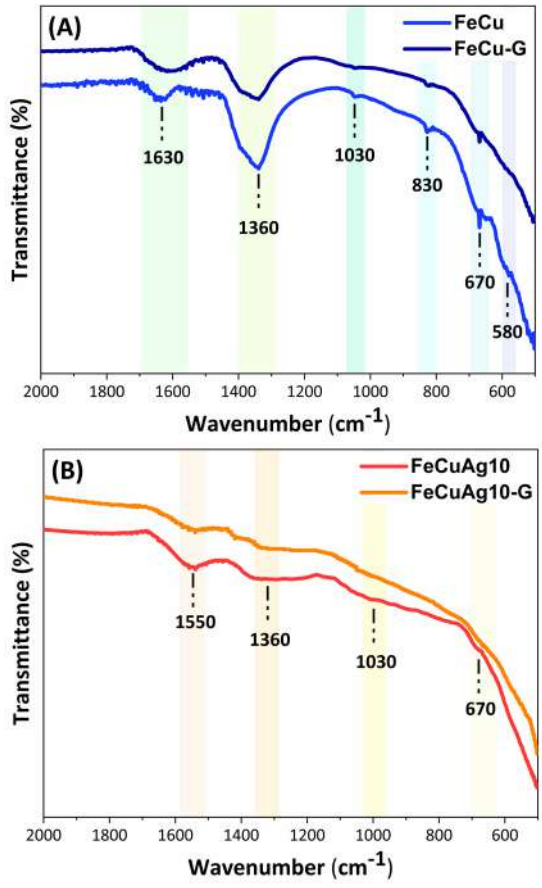

Figure 1. FTIR spectra of FeCu and FeCu-G (**A**) and FeCuAg10 and FeCuAg10-G samples (**B**)

Other authors have documented the variations between coated materials' IR spectra and those of uncoated or non-functionalized materials (**Chitradevi *et al.***, 2019; **Kumar *et al.***, 2019; **Singh *et al.***, 2022), which can be attributed to the surface interaction of phytochemicals present in the extract. Literature reports demonstrate that polyphenols, flavonoids, proteins, and organic acids, including O–H, N–H, and C=O groups, adsorb onto metallic or oxide surfaces during biogenic synthesis, leading to shifts or intensity changes in FTIR peaks (**Kumar *et al.***, 2016). Furthermore, any variation in particle size or morphology induced by the extract may enhance surface area effects, amplifying the superficial functional groups as observed in O–H bound spectral changes.

On the other hand, the XRD pattern of the non-functionalized NPs (**Figure 2**) shows six peaks in the whole spectrum, with 2θ values of 35.62°, 36.42°, 38.80°, 42.30°, 61.44°, and 73.52° for the FeCu and FeCu-G samples. Using the X'pert high score Plus software and the Crystallography Open Database (COD), these signals were assigned to three crystalline phases: a first phase of iron (III) oxide (Fe_2O_3) (ICDD 01-073-2234), presenting a rhombohedral structure with space group R3-C (167), lattice parameters a = b = 5.0342 Å and c = 13.7483 Å, with angles α = β = 90° and γ = 120°, a relative abundance of 95% in FeCu and 93% in FeCu-G; a second phase of copper(I) oxide or (Cu_2O) (ICDD 01-078-2076) with cubic structure and space group Pn-3m (224), lattice parameters $a = b = c =$ 4.2670 Å with angles α = β = γ = 90°, and a relative abundance of 3% in FeCu and 6% in FeCu-G, with the use of guava fruit extract increasing the formation of Cu_2O, and a last phase of copper(II) oxide (CuO) (ICDD 01-089-2529) with a monoclinic structure and space group C2/c (15), lattice parameters a = 4.6853 Å, b = 3.4257 Å, c = 5.1303 Å of angles α = γ = 90°, β = 99.549°, relative abundance of 2% in FeCu and 1% in FeCu-G, a

reduction due to the reactions generated by the multicomponent matrix of guava extract, transforming and stabilizing the Cu^{2+} ions into Cu^{1+}. These results agree with other reports (**Mohamed *et al.***, 2021; **Parvathiraja & Shailajha**, 2021).

The XRD spectra of silver functionalized nanocomposites (**Figure 3**) revealed peaks of both the nanocomposite support and the immobilized Ag NPs; the signals corresponded to an Ag phase with 2θ values of 38.18°, 44.38°, 64.52°, and 77.50° matching crystallographic planes (111), (200), (220), and (311), respectively, and exhibiting a cubic structure with space group *Fm-3m* (225), lattice parameters $a = b = c = 4.0773$ Å, and angles $\alpha = \beta = \gamma = 90°$. The peaks assigned to the NPs showed lower intensity compared to their non-functionalized counterparts, which has been attributed to the presence of Ag-NPs on the

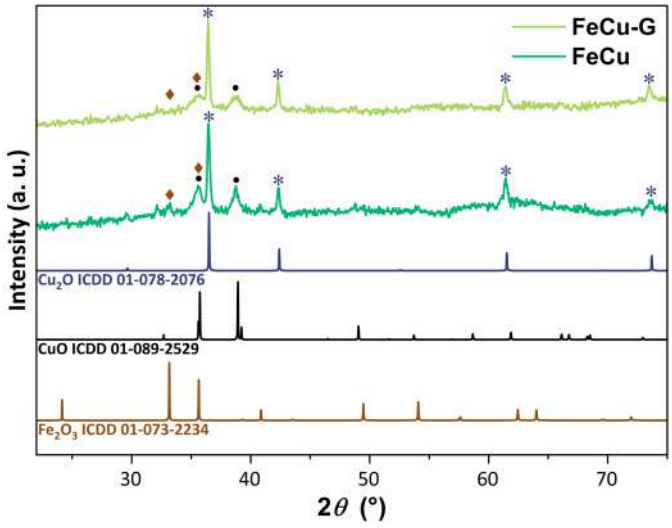

Figure 2. XRD patterns of the unfunctionalized FeCu and FeCu-G samples. The peaks assigned to the detected crystalline phases are indicated with the symbols (*) Cu_2O, (◊) Fe_2O_3, and (•) CuO

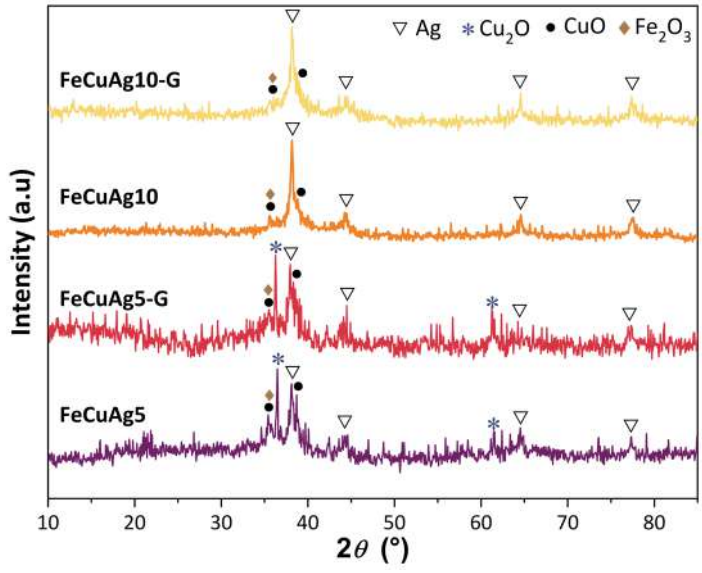

Figure 3. XRD of functionalized samples. The peaks assigned to the Ag crystalline phases are indicated with the symbol (∇). The peaks observed in the diffractograms indicate the crystalline nature of the synthesized solids

Revista de la Academia Colombiana de Ciencias Exactas, Físicas y Naturales
49(193):818-832, octubre-diciembre de 2025. doi: https://doi.org/10.18257/raccefyn.3187

surface of the nanocomposites (**Kanwal *et al.***, 2019), where the absence of specific peaks in the diffractograms of the functionalized samples may respond to the higher concentration of Ag-NPs.

The reducing and stabilizing capacity of the guava extract can be attributed directly to its phytochemical composition. Previous studies have demonstrated that *P. guajava* is rich in bioactive metabolites such as flavonoids, polyphenols, tannins, carotenoids, and ascorbic acid, all of which exhibit well-documented redox activity and surface-capping ability in green synthesis routes (**Nguyen *et al.***, 2023; **Otálora *et al.***, 2022, 2024). These compounds may actively contribute to nanoparticle nucleation, growth regulation, and surface stabilization, while also enhancing the antibacterial functionality of the resulting nanocomposites. Although we did not evaluate here the influence of the guava variety, ripening stage, or agroecological conditions on the composition of the extract, these factors are known to affect the concentration and stability of bioactive molecules (**Ibrahim *et al.***, 2019; **Nguyen *et al.***, 2023).

These structural modifications are not only indicative of the successful silver functionalization and the interaction of phytochemicals with the oxide-based composite surface, but they also have direct implications for the antibacterial behavior of the nanocomposites. Previous studies have shown that silver-functionalized copper and iron oxides exhibit enhanced antibacterial performance due to a synergistic mechanism where structural defects, exposed surface functional groups (–OH, –NH), and Ag-related surface reactivity facilitate reactive oxygen species (ROS) generation and membrane disruption in Gram-negative bacteria (**Antonoglou *et al.***, 2019; **Pareek *et al.***, 2021; **Parvathiraja & Shailajha**, 2021).

Structural morphological analyses

The TEM and HR-TEM images of the FeCuAg5-G nanocomposite are shown in **Figure 4A-D**. Agglomerated nanosized crystals can be observed in these images (**A**, **C**), a common characteristic of polycrystalline materials (**Abd El-Sadek *et al.***, 2019). The morphology of the compounds analyzed is circular and heterogeneous, and the contrasts observed in the images arise due to the different orientations of the crystals in relation to the electron beam (**Yalcin *et al.***, 2014). The particles observed have diameters ranging between 7.10 nm and 19.40 nm, with an average diameter of 7.69 ± 0.57 nm. The lattice lines correspond to the interplanar distances in **Figure 4B**, which were calculated using HR-TEM and measured on a 10 nm scale. The highly crystalline structure with an interplanar distance of d = 0.25 nm on the plane (002), consistent with the monoclinic phase of CuO, matched the XRD data and reports (**Pallavolu *et al.***, 2023). On the other hand, it was possible to observe the silver nanoparticles with a defined spherical shape (**Figure 4D**).

Sample FeCuAg10 SEM image (**Figure 5 A-B**) shows aggregates without a specific shape, with an average particle size of 103.7 ± 7.3 nm. In contrast, sample FeCuAg10-G (**Figure 5 C-D**) had nanoflakes structures with defined edges and smooth surfaces (79.54 ± 4.41 nm). This flake morphology is attributed to the presence of copper oxide CuO (**Siddiqui *et al.***, 2016), so the elongated CuO distribution corresponds to the preferential orientation of this oxide along the crystallographic plane (010) (**Hwa *et al.***, 2019; **Pallavolu *et al.***, 2023). The spherical particles in both samples are due to Ag NPs, while the other heterogeneous phase is attributed to the Fe_2O_3 phase.

Magnetic characterization

Figure 6 shows the magnetization vs field isotherm at 300 K for FeCuAg10 and FeCuAg10-G samples. The coercivity field (H_c) and remanent magnetization (M_r) (**Gaona *et al.***, 2023; **Saavedra-Gaona *et al.***, 2024) were determined for FeCuAg10, with M_r = 0.0011 emu/g and H_c = 11 Oe, and for FeCuAg10-G, with M_r = 0.00034 emu/g and Hc = 5 Oe. The hysteresis loops depict weak ferromagnetic behavior with a predominant paramagnetic contribution. This behavior is attributed to particle size reductions, oxygen vacancies, and spin ordering (**Atchaya & Meena Devi**, 2024). Additionally, nanostructure anisotropy, oxygen vacancies, structural disorder, defects, surface spins, and magnetic exchange coupling contribute to these properties (**Al-Saeedi *et al.***, 2021; **Atchaya & Meena Devi**, 2024; **Batsaikhan *et al.***, 2020).

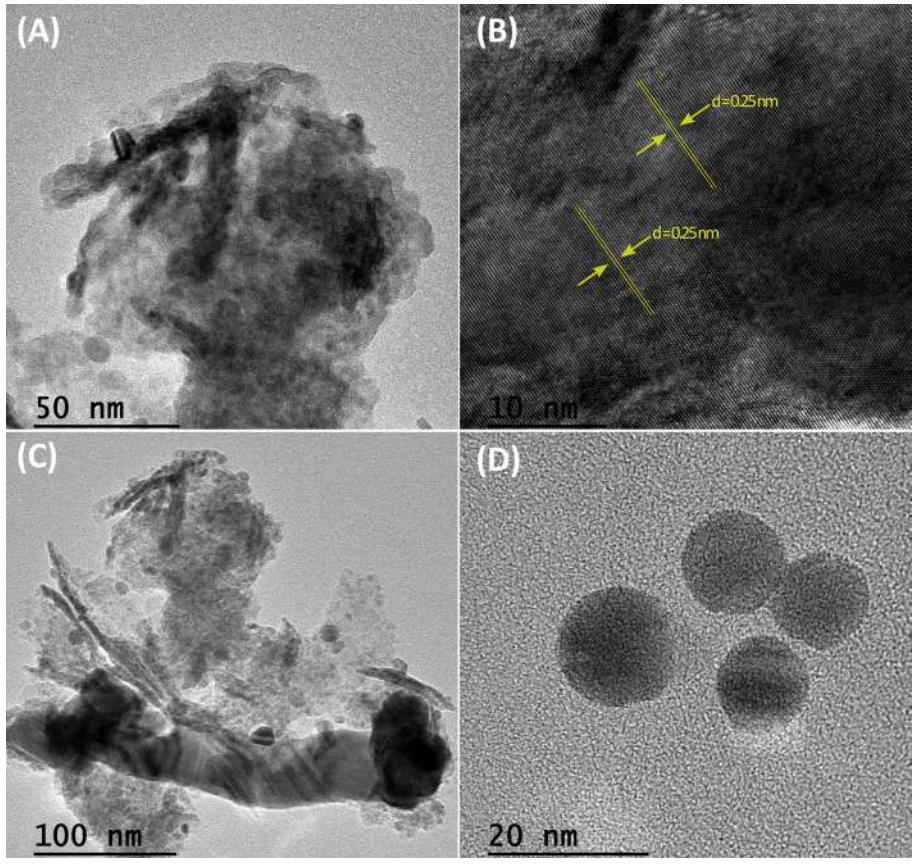

Figure 4. TEM and HR-TEM images of the FeCuAg5-G sample. The TEM images display polycrystalline agglomerates with spherical shape, whereas the HR-TEM analysis reveals a d-distance value of ~ 0.25 nm

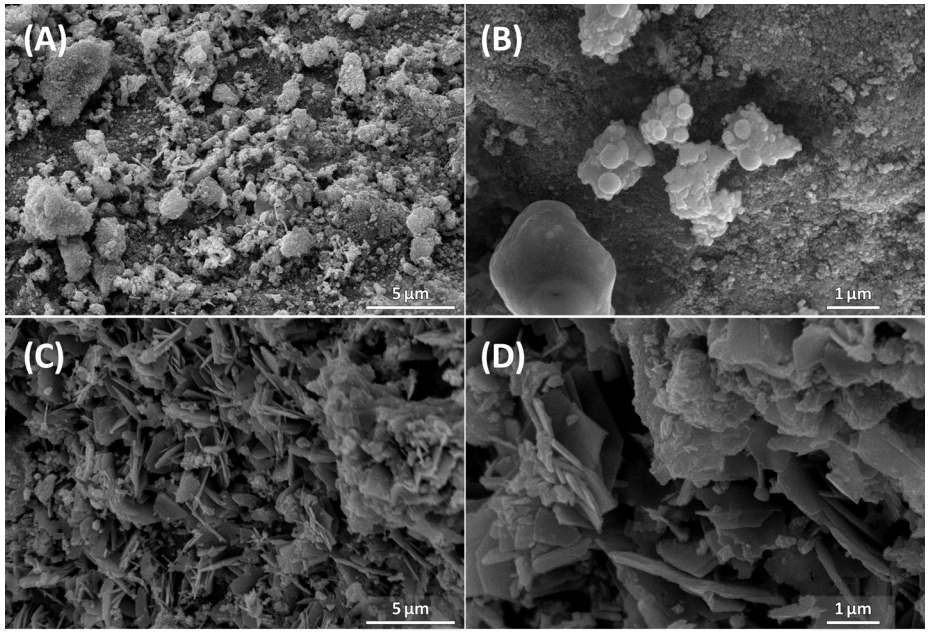

Figure 5. SEM images for the FeCuAg10 (A-B) and FeCuAg10-G (C-D) samples

Revista de la Academia Colombiana de Ciencias Exactas, Físicas y Naturales
49(193):818-832, octubre-diciembre de 2025. doi: https://doi.org/10.18257/raccefyn.3187

Bactericidal activity

The microdilution tests evaluated the bactericidal activity of the synthesized nanocomposites against the Gram-negative *K. pneumoniae* strain. Bacterial growth inhibition percentages for different nanocomposite concentrations are presented in **Figure 7**; the maximum bacterial growth inhibitory capacity of functionalized and non-functionalized

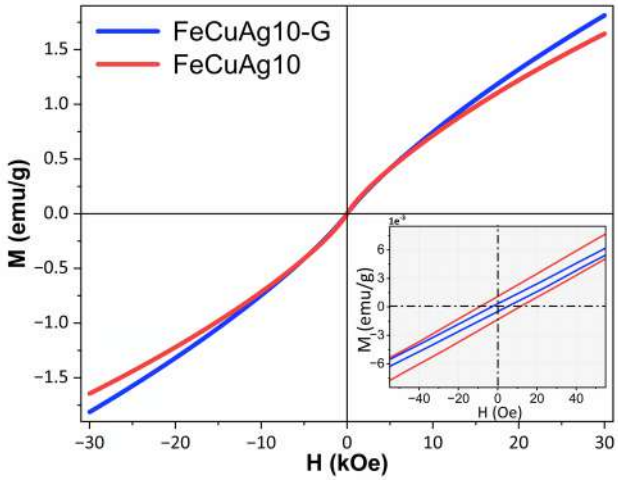

Figure 6. Magnetic isotherms at 300 K of FeCuAg10 and FeCuAg10-G samples

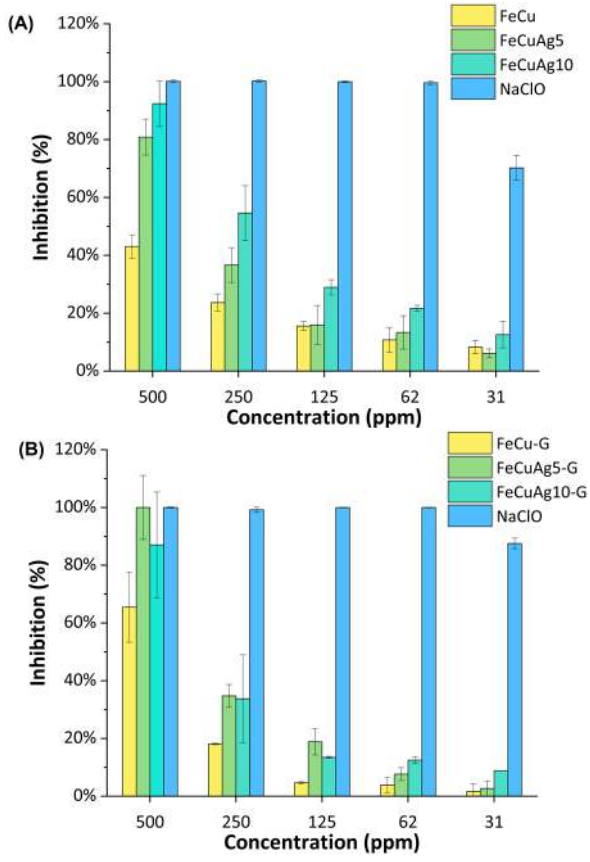

Figure 7. Bactericidal response against *Klebsiella pneumoniae*

nanocomposites occurred at 500 ppm, in contrast with the NaClO positive target 7% concentration (70,000 ppm). The bactericidal potential of the nanocomposites against the target was evident, which is even more relevant when considering the high resistance prevalence rates of this bacterium against most commonly used antimicrobial drugs, including cefepime, aztreonam, and cefotaxime, with 72.6%, 73.3%, and 79.2%, respectively (**Effah *et al.***, 2020).

Although the microdilution tests showed an inhibitory effect on bacterial growth for all nanocomposites, it was higher in the functionalized samples, probably explained by the fact that Fe_2O_3 NPs, for example, tend to exhibit greater bactericidal activity against Gram-positive bacteria than against Gram-negative bacteria, which is attributed to the fact that these NPs are highly stable under normal environmental conditions, thus generating fewer metal ions releases that exert bactericidal activity (**Pallela *et al.***, 2019). On the other hand, **Parek *et al.*** (2021) explained how bactericidal response improvement in functionalized solids is due to Ag NPs generating intra- and extracellular ROS in *K. pneumoniae*, which, consequently, produces oxidative stress leading to cellular demise. Also, Ag NPs can damage bacterial DNA and inhibit microbial growth by releasing Ag^+ ions, which interact with sulfur compounds, leading to cell death. (**Shahriary *et al.***, 2018).

Conclusions

The structural characterization confirmed the synthesis of copper oxide and iron oxide functionalized with silver NPs. The use of guava fruit extract not only modified the phase composition, increasing the presence of Cu_2O, but also promoted the formation of nanoflake-like morphologies, highlighting its role as a sustainable capping and reducing agent. Magnetic evaluation revealed predominantly paramagnetic behavior with weak ferromagnetic contributions. Notably, the incorporation of the extract led to reduced saturation magnetization and coercivity, evidencing the influence of phytochemicals on the magnetic response. Besides, the biogenic route enhanced the antibacterial activity of the nanocomposites, as functionalized samples synthesized with guava extract exhibited stronger inhibition against *K. pneumoniae*. These findings demonstrate that green synthesis using guava extract provides a viable pathway for tailoring structural, magnetic, and antibacterial properties, underscoring its potential for biomedical and environmental applications.

Acknowledgements

We thank the research departments at Universidad Pedagógica y Tecnológica de Colombia and Universidad Antonio Nariño (Project No. 2022205) for their support in the realization of this work.

Author contributions

CAPV, RJRO: supervision. **MCM, GLMN:** material preparation. **CCRF, CLSS, IMSG**: characterization. **MCM, GLMN, RJRO, IMSG, DLLP**: methodology and formal analysis. **MCM, GLMN:** drafting of the initial manuscript. All authors conducted conceptualization and investigation, and reviewed and approved the final manuscript.

Conflicts of interest

The authors declare there are no conflicts of interest regarding the publication of this article. They also declare that they have no financial or personal relationships that could influence their work or affect the interpretation of the results presented in this article

References

Abd El-Sadek, M. S., Wasly, H. S., Batoo, K. M. (2019). X-ray peak profile analysis and optical properties of CdS nanoparticles synthesized via the hydrothermal method. *Applied Physics A*, *125*(4), 283. https://doi.org/10.1007/s00339-019-2576-y

Akin, S., Sadegh, F., Turan, S., Sonmezoglu, S. (2019). Inorganic CuFeO2 Delafossite Nanoparticles as Effective Hole Transport Materials for Highly Efficient and Long-Term Stable Perovskite Solar Cells. *ACS Applied Materials & Interfaces*, *11*(48), 45142-45149. https://doi.org/10.1021/acsami.9b14740

Aksu Demirezen, D., Yıldız, Y. Ş., Yılmaz, Ş., Demirezen Yılmaz, D. (2019). Green synthesis and characterization of iron oxide nanoparticles using *Ficus carica* (common fig) dried fruit extract. *Journal of Bioscience and Bioengineering*, *127*(2), 241-245. https://doi.org/10.1016/j.jbiosc.2018.07.024

Al-Saeedi, S. I., Al-Senani, G. M., Abd-Elkader, O. H., Deraz, N. M. (2021). One Pot Synthesis, Surface and Magnetic Properties of Cu2O/Cu and Cu2O/CuO Nanocomposites. *Crystals*, *11*(7), Article 7. https://doi.org/10.3390/cryst11070751

Al-Senani, G. M., Al-Saeedi, S. I., Al-Kadhi, N. S., Abd-Elkader, O. H., Deraz, N. M. (2022). Green Synthesis and Pinning Behavior of Fe-Doped CuO/Cu2O/Cu4O3 Nanocomposites. *Processes*, *10*(4), Article 4. https://doi.org/10.3390/pr10040729

Altammar, K. A. (2023). A review on nanoparticles: characteristics, synthesis, applications, and challenges. *Frontiers in Microbiology*, *14*, 1155622. https://doi.org/10.3389/fmicb.2023.1155622

Amin, N. H., Ali, L. I., El-Molla, S. A., Ebrahim, A. A., Mahmoud, H. R. (2016). Effect of Fe2O3 precursors on physicochemical and catalytic properties of CuO/Fe2O3 system. *Arabian Journal of Chemistry*, *9*, S678-S684. https://doi.org/10.1016/j.arabjc.2011.07.026

Antonoglou, O., Lafazanis, K., Mourdikoudis, S., Vourlias, G., Lialiaris, T., Pantazaki, A., Dendrinou-Samara, C. (2019). Biological relevance of CuFeO2 nanoparticles: Antibacterial and anti-inflammatory activity, genotoxicity, DNA and protein interactions. *Materials Science and Engineering: C*, *99*, 264-274. https://doi.org/10.1016/j.msec.2019.01.112

Apte, S. K., Naik, S. D., Sonawane, R. S., Kale, B. B., Baeg, J. O. (2007). Synthesis of Nanosize-Necked Structure α- and γ-Fe2O3 and its Photocatalytic Activity. *Journal of the American Ceramic Society*, *90*(2), 412-414. https://doi.org/10.1111/j.1551-2916.2006.01424.x

Arsiya, F., Sayadi, M. H., Sobhani, S. (2017). Green synthesis of palladium nanoparticles using *Chlorella vulgaris*. *Materials Letters*, *186*, 113-115. https://doi.org/10.1016/j.matlet.2016.09.101

Atchaya, S. & Meena Devi, J. (2024). Experimental Investigation on Structural, Optical, Electrical and Magnetic Properties of Copper Oxide Nanoparticles. *Proceedings of the National Academy of Sciences, India Section A: Physical Sciences*, *94*(1), 153-160. https://doi.org/10.1007/s40010-023-00855-7

Ayala, A. B. (2017). Agrobiodiversity and nutrition in Boyacá, Colombia: a historic relationship of imbalance. *Cultura Científica*, *15*, Article 15.

Batsaikhan, E., Lee, C.-H., Hsu, H., Wu, C.-M., Peng, J.-C., Ma, M.-H., Deleg, S., Li, W.-H. (2020). Largely Enhanced Ferromagnetism in Bare CuO Nanoparticles by a Small Size Effect. *ACS Omega*, *5*(8), 3849-3856. https://doi.org/10.1021/acsomega.9b02913

Bhavyasree, P. G. & Xavier, T. S. (2020). Green synthesis of Copper Oxide/Carbon nanocomposites using the leaf extract of *Adhatoda vasica* Nees, their characterization and antimicrobial activity. *Heliyon*, *6*(2), e03323. https://doi.org/10.1016/j.heliyon.2020.e03323

Bhushan, M., Kumar, Y., Periyasamy, L., Viswanath, A. K. (2019). Study of synthesis, structural, optical and magnetic characterizations of iron/copper oxide nanocomposites: A promising novel inorganic antibiotic. *Materials Science and Engineering: C*, *96*, 66-76. https://doi.org/10.1016/j.msec.2018.11.009

Buarki, F., AbuHassan, H., Al Hannan, F., Henari, F. Z. (2022). Green Synthesis of Iron Oxide Nanoparticles Using *Hibiscus rosa sinensis* Flowers and their Antibacterial Activity. *Journal of Nanotechnology*, *2022*, e5474645. https://doi.org/10.1155/2022/5474645

Buledi, J. A., Pato, A. H., Kanhar, A. H., Solangi, A. R., Batool, M., Ameen, S., Palabiyik, I. M. (2021). Heterogeneous kinetics of CuO nanoflakes in simultaneous decolorization of Eosin Y and Rhodamine B in aqueous media. *Applied Nanoscience*, *11*, 1241-1256. https://doi.org/10.1007/s13204-021-01685-y

Cahyana, A. H., Liandi, A. R., Yulizar, Y., Romdoni, Y., Wendari, T. P. (2021). Green synthesis of CuFe2O4 nanoparticles mediated by *Morus alba* L. leaf extract: Crystal structure, grain morphology, particle size, magnetic and catalytic properties in Mannich reaction. *Ceramics International*, *47*(15), 21373-21380. https://doi.org/10.1016/j.ceramint.2021.04.146

Castañeda-Mendoza, M., Parra-Vargas, C. A., Rincón-Joya, M., Chiquito, A. J., Raba-Páez, A. M. (2025). Gas Sensor Properties of (CuO/WO3)-CuWO4 Heterostructured Nanocomposite Materials. *Materials*, *18*(12), 2896. https://doi.org/10.3390/ma18122896

Charbgoo, F., Ahmad, M. B., Darroudi, M. (2017). Cerium oxide nanoparticles: green synthesis and biological applications. *International Journal of Nanomedicine*, *12*, 1401-1413. https://doi.org/10.2147/IJN.S124855

Chitradevi, T., Lenus, A. J., Jaya, N. V. (2019). Structure, morphology and luminescence properties of sol-gel method synthesized pure and Ag-doped ZnO nanoparticles. *Materials Research Express*, *7*(1), 015011. https://doi.org/10.1088/2053-1591/ab5c53

Chokkareddy, R. & Redhi, G. G. (2018). Green Synthesis of Metal Nanoparticles and its Reaction Mechanisms. In *Green Metal Nanoparticles* (pp. 113-139). John Wiley & Sons, Ltd. https://doi.org/10.1002/9781119418900.ch4

Effah, C. Y., Sun, T., Liu, S., Wu, Y. (2020). *Klebsiella pneumoniae*: an increasing threat to public health. *Annals of Clinical Microbiology and Antimicrobials*, *19*(1), 1. https://doi.org/10.1186/s12941-019-0343-8

El-Boubbou, K., Ali, R., Bahhari, H. M., AlSaad, K. O., Nehdi, A., Boudjelal, M., AlKushi, A. (2016). Magnetic Fluorescent Nanoformulation for Intracellular Drug Delivery to Human Breast Cancer, Primary Tumors, and Tumor Biopsies: Beyond Targeting Expectations. *Bioconjugate Chemistry*, *27*(6), 1471-1483. https://doi.org/10.1021/acs.bioconjchem.6b00257

Fakhari, S., Jamzad, M., Kabiri Fard, H. (2019). Green synthesis of zinc oxide nanoparticles: a comparison. *Green Chemistry Letters and Reviews*, *12*(1), 19-24. https://doi.org/10.1080/17518253.2018.1547925

Gaona, I. M. S., Mendoza, M. C., Vargas, C. A. P. (2023). Structural and Magnetic Properties of Nd3Ba5Cu8O18+δ Superconductor. *Journal of Low Temperature Physics*, *211*(3), 156-165. https://doi.org/10.1007/s10909-023-02963-5

Hwa, K. Y., Karuppaiah, P., Gowthaman, N. S. K., Balakumar, V., Shankar, S., Lim, H. N. (2019). Ultrasonic synthesis of CuO nanoflakes: A robust electrochemical scaffold for the sensitive detection of phenolic hazard in water and pharmaceutical samples. *Ultrasonics Sonochemistry*, *58*, 104649. https://doi.org/10.1016/j.ultsonch.2019.104649

Ibrahim, E. H., Kilany, M., Ghramh, H. A., Khan, K. A., ul Islam, S. (2019). Cellular proliferation/cytotoxicity and antimicrobial potentials of green synthesized silver nanoparticles (AgNPs) using *Juniperus procera*. *Saudi Journal of Biological Sciences*, *26*(7), 1689-1694. https://doi.org/10.1016/j.sjbs.2018.08.014

Ismail, M. I. M. (2020). Green synthesis and characterizations of copper nanoparticles. *Materials Chemistry and Physics*, *240*, 122283. https://doi.org/10.1016/j.matchemphys.2019.122283

Jacob, S. J. P., Prasad, V. L. S., Sivasankar, S., Muralidharan, P. (2017). Biosynthesis of silver nanoparticles using dried fruit extract of *Ficus carica* - Screening for its anticancer activity and toxicity in animal models. *Food and Chemical Toxicology*, *109*, 951-956. https://doi.org/10.1016/j.fct.2017.03.066

Jadoun, S., Arif, R., Jangid, N. K., Meena, R. K. (2021). Green synthesis of nanoparticles using plant extracts: a review. *Environmental Chemistry Letters*, *19*(1), 355-374. https://doi.org/10.1007/s10311-020-01074-x

Jamzad, M. & Bidkorpeh, M. (2020). Green synthesis of iron oxide nanoparticles by the aqueous extract of *Laurus nobilis* L. leaves and evaluation of the antimicrobial activity. *Journal of Nanostructure in Chemistry*, *10*. https://doi.org/10.1007/s40097-020-00341-1

Jansanthea, P., Inyai, N., Chomkitichai, W., Ketwaraporn, J., Ubolsook, P., Wansao, C., Wanaek, A., Wannawek, A., Kuimalee, S., Pookmanee, P. (2024). Green synthesis of CuO/Fe2O3/ZnO ternary composite photocatalyst using grape extract for enhanced photodegradation of environmental organic pollutant. *Chemosphere*, *351*, 141212. https://doi.org/10.1016/j.chemosphere.2024.141212

Johurul Islam, M., Khatun, N., Hossen Bhuiyan, R., Sultana, S., Shaikh, M. A. A., Bitu, M. N. A., Chowdhury, F., Islam, S. (2023). *Psidium guajava* leaf extract mediated green synthesis of silver nanoparticles and its application in antibacterial coatings. *RSC Advances*, *13*(28), 19164-19172. https://doi.org/10.1039/D3RA03381C

Jose, J., Kumar, R., Harilal, S., Mathew, G. E., Parambi, D. G. T., Prabhu, A., Uddin, Md. S., Aleya, L., Kim, H., Mathew, B. (2020). Magnetic nanoparticles for hyperthermia in cancer treatment: an emerging tool. *Environmental Science and Pollution Research*, *27*(16), 19214-19225. https://doi.org/10.1007/s11356-019-07231-2

Kanwal, Z., Raza, M. A., Riaz, S., Manzoor, S., Tayyeb, A., Sajid, I., Naseem, S. (2019). Synthesis and characterization of silver nanoparticle-decorated cobalt nanocomposites (Co@AgNPs) and their density-dependent antibacterial activity. *Royal Society Open Science*, *6*(5), 182135. https://doi.org/10.1098/rsos.182135

Khalil, A. T., Ovais, M., Ullah, I., Ali, M., Shinwari, Z. K., Maaza, M. (2017). Biosynthesis of iron oxide (Fe2O3) nanoparticles via aqueous extracts of *Sageretia thea* (Osbeck.) and their pharmacognostic properties. *Green Chemistry Letters and Reviews*, *10*(4), 186-201. https://doi.org/10.1080/17518253.2017.1339831

Kooti, M., Saiahi, S., Motamedi, H. (2013). Fabrication of silver-coated cobalt ferrite nanocomposite and the study of its antibacterial activity. *Journal of Magnetism and Magnetic Materials*, *333*, 138-143. https://doi.org/10.1016/j.jmmm.2012.12.038

Kumar, B., Smita, K., Cumbal, L., Debut, A. (2017). Green synthesis of silver nanoparticles using Andean blackberry fruit extract. *Saudi Journal of Biological Sciences*, *24*(1), 45-50. https://doi.org/10.1016/j.sjbs.2015.09.006

Kumar Das, P., Mohanty, C., Krishna Purohit, G., Mishra, S., Palo, S. (2022). Nanoparticle assisted environmental remediation: Applications, toxicological implications and recommendations for a sustainable environment. *Environmental Nanotechnology, Monitoring & Management*, *18*, 100679. https://doi.org/10.1016/j.enmm.2022.100679

Kumar, K. K. P., Dinesh, N. D., Murari, S. K. (2019). Synthesis of CuO and Ag doped CuO nanoparticles from Muntingia calabura leaf extract and evaluation of their antimicrobial potential. *International Journal of Nano and Biomaterials*, *8*(3-4), 228-252. https://doi.org/10.1504/IJNBM.2019.104939

Mahfuzul Hoque, M. D., Bari, M. L., Inatsu, Y., Juneja, V. K., Kawamoto, S. (2007). Antibacterial activity of guava (*Psidium guajava* L.) and Neem (*Azadirachta indica* A. Juss.) extracts against foodborne pathogens and spoilage bacteria. *Foodborne Pathogens and Disease*, *4*(4), 481-488. https://doi.org/10.1089/fpd.2007.0040

Manikandan, R. & Anand, V. (2015). A Review on Antioxidant activity of *Psidium guajava*. *Research Journal of Pharmacy and Technology*, *8*, 339. https://doi.org/10.5958/0974-360X.2015.00056.6

Marslin, G., Siram, K., Maqbool, Q., Selvakesavan, R. K., Kruszka, D., Kachlicki, P., Franklin, G. (2018). Secondary Metabolites in the Green Synthesis of Metallic Nanoparticles. *Materials*, *11*(6), Article 6. https://doi.org/10.3390/ma11060940

Mohamed, H. E. A., Thema, T., Dhlamini, M. S. (2021). Green synthesis of CuO nanoparticles via *Hyphaene thebaica* extract and their optical properties. *Materials Today: Proceedings*, *36*, 591-594. https://doi.org/10.1016/j.matpr.2020.05.592

Naik, T. S. S. K., Singh, S., Narasimhappa, P., Varshney, R., Singh, J., Khan, N. A., Zahmatkesh, S., Ramamurthy, P. C., Shehata, N., Kiran, G. N., Sunil, K. (2023). Green and sustainable synthesis of CaO nanoparticles: Its solicitation as a sensor material and electrochemical detection of urea. *Scientific Reports*, *13*(1), 19995. https://doi.org/10.1038/s41598-023-46728-2

Narayanan, M., Divya, S., Natarajan, D., Senthil-Nathan, S., Kandasamy, S., Chinnathambi, A., Alahmadi, T. A., Pugazhendhi, A. (2021). Green synthesis of silver nanoparticles from aqueous extract of *Ctenolepis garcini* L. and assess their possible biological applications. *Process Biochemistry*, *107*, 91-99. https://doi.org/10.1016/j.procbio.2021.05.008

Nguyen, D.-K., Hung, N. Q., Dinh, V.-P. (2023). Antibacterial properties of silver nanoparticles greenly synthesized using guava fruit extract as a reducing agent and stabilizer. *Applied Nanoscience*, *13*(6), 3709-3720. https://doi.org/10.1007/s13204-022-02506-6

Nope, E., Sathicq, G., Martínez, J. J., Gaona, I. M. S., Mendoza, M. C., Vargas, C. A. P., Romanelli, G. P., Luque, R. (2025). Cationic charge influence on the magnetic response of the Fe3O4–[Me2+ 1−y Me3+ y (OH2)] y+(Co3 2−) y/2·mH2O hydrotalcite system. *Nanotechnology Reviews*, *14*(1). https://doi.org/10.1515/ntrev-2025-0204

Otálora, M. C., Wilches-Torres, A., Gómez-Castaño, J. A. (2022). Spray-Drying Microencapsulation of Pink Guava (Psidium guajava) Carotenoids Using Mucilage from Opuntia ficus-indica Cladodes and Aloe Vera Leaves as Encapsulating Materials. *Polymers*, *14*(2), 310. https://doi.org/10.3390/polym14020310

Otálora, M. C., Wilches-Torres, A., Gómez-Castaño, J. A. (2024). Physicochemical and bioactive characterization of pink guava pulp microcapsules prepared by freeze-drying using coffee mucilage as a wall material. *LWT*, *207*, 116665. https://doi.org/10.1016/j.lwt.2024.116665

Paidari, S. & Ibrahim, S. A. (2021). Potential application of gold nanoparticles in food packaging: a mini review. *Gold Bulletin*, *54*(1), 31-36. https://doi.org/10.1007/s13404-021-00290-9

Pallavolu, M.-R., Banerjee, A.-N., Joo, S.-W. (2023). Battery-Type Behavior of Al-Doped CuO Nanoflakes to Fabricate a High-Performance Hybrid Supercapacitor Device for Superior Energy Storage Applications. *Coatings*, *13*(8), Article 8. https://doi.org/10.3390/coatings13081337

Pallela, P. N. V. K., Ummey, S., Ruddaraju, L. K., Gadi, S., Cherukuri, C. S., Barla, S., Pammi, S. V. N. (2019). Antibacterial efficacy of green synthesized α-Fe2O3 nanoparticles using Sida cordifolia plant extract. *Heliyon*, *5*(11), e02765. https://doi.org/10.1016/j.heliyon.2019.e02765

Pareek, V., Devineau, S., Sivasankaran, S. K., Bhargava, A., Panwar, J., Srikumar, S., Fanning, S. (2021). Silver Nanoparticles Induce a Triclosan- Like Antibacterial Action Mechanism in Multi-Drug Resistant *Klebsiella pneumoniae*. *Frontiers in Microbiology*, *12*, 638640. https://doi.org/10.3389/fmicb.2021.638640

Parvathiraja, C. & Shailajha, S. (2021). Bioproduction of CuO and Ag/CuO heterogeneous photocatalysis-photocatalytic dye degradation and biological activities. *Applied Nanoscience*, *11*(4), 1411-1425. https://doi.org/10.1007/s13204-021-01743-5

Parvekar, P., Palaskar, J., Metgud, S., Maria, R., Dutta, S. (2020). The minimum inhibitory concentration (MIC) and minimum bactericidal concentration (MBC) of silver nanoparticles against *Staphylococcus aureus*. *Biomaterial Investigations in Dentistry*, *7*(1), 105-109. https://doi.org/10.1080/26415275.2020.1796674

Patil, S. P. & Rane, P. M. (2020). *Psidium guajava* leaves assisted green synthesis of metallic nanoparticles: a review. *Beni-Suef University Journal of Basic and Applied Sciences*, *9*(1), 60. https://doi.org/10.1186/s43088-020-00088-2

Rajesh Kumar, T. V., Murthy, J. S. R., Narayana Rao, M., Bhargava, Y. (2016). Evaluation of silver nanoparticles synthetic potential of *Couroupita guianensis* Aubl., flower buds extract and their synergistic antibacterial activity. *3 Biotech*, *6*(1), 92. https://doi.org/10.1007/s13205-016-0407-9

Ramola, B., Joshi, N. C., Ramola, M., Chhabra, J., Singh, A. (2019). Green Synthesis, Characterisations and Antimicrobial Activities of CaO Nanoparticles. *Oriental Journal of Chemistry*, *35*(3), 1154-1157.

Rashid, S. S., Mustafa, A. H., Ab Rahim, M. H. (2022). Ferromagnetic nanoparticles synthesis and functionalization for laccase enzyme immobilization. *Materials Today: Proceedings*, *48*, 916-919. https://doi.org/10.1016/j.matpr.2021.03.661

Reddy, K. R. (2017). Green synthesis, morphological and optical studies of CuO nanoparticles. *Journal of Molecular Structure*, *1150*, 553-557. https://doi.org/10.1016/j.molstruc.2017.09.005

Rodríguez-Medina, N. N. & Valdés-Infante Herrero, J. (2016). Chapter 13 - Guava (*Psidium guajava* L.) Cultivars: An Important Source of Nutrients for Human Health. In M. S. J. Simmonds & V. R. Preedy (Eds.), *Nutritional Composition of Fruit Cultivars* (pp. 287-315). Academic Press. https://doi.org/10.1016/B978-0-12-408117-8.00013-1

Saavedra-Gaona, I. M., Supelano, G. I., Suárez-Vera, S. G., Fonseca, L. C. I., Castañeda-Mendoza, M., Sánchez-Sáenz, C. L., Izquierdo, J. L., Gómez, A., Morán, O., Parra-Vargas, C. A. (2024). Magnetic and electrical behaviour of Yb substitution on Bi1-*x*Yb*x*FeO3 ($0.00 < x < 0.06$) ceramic system. *Journal of Magnetism and Magnetic Materials*, *593*, 171827. https://doi.org/10.1016/j.jmmm.2024.171827

Salem, S. S., EL-Belely, E. F., Niedbała, G., Alnoman, M. M., Hassan, S. E.-D., Eid, A. M., Shaheen, T. I., Elkelish, A., Fouda, A. (2020). Bactericidal and In-Vitro Cytotoxic Efficacy of Silver Nanoparticles (Ag-NPs) Fabricated by Endophytic Actinomycetes and Their Use as Coating for the Textile Fabrics. *Nanomaterials*, *10*(10), Article 10. https://doi.org/10.3390/nano10102082

Santhoshkumar, T., Rahuman, A. A., Jayaseelan, C., Rajakumar, G., Marimuthu, S., Kirthi, A. V., Velayutham, K., Thomas, J., Venkatesan, J., Kim, S.-K. (2014). Green synthesis of titanium dioxide nanoparticles using *Psidium guajava* extract and its antibacterial and antioxidant properties. *Asian Pacific Journal of Tropical Medicine*, *7*(12), 968-976. https://doi.org/10.1016/S1995-7645(14)60171-1

Shahriary, M., Veisi, H., Hekmati, M., Hemmati, S. (2018). In situ green synthesis of Ag nanoparticles on herbal tea extract (Stachys lavandulifolia)-modified magnetic iron oxide nanoparticles as antibacterial agent and their 4-nitrophenol catalytic reduction activity. *Materials Science and Engineering: C*, *90*, 57-66. https://doi.org/10.1016/j.msec.2018.04.044

Sharma, D., Ledwani, L., Mehrotra, T., Kumar, N., Pervaiz, N., Kumar, R. (2020). Biosynthesis of hematite nanoparticles using *Rheum emodi* and their antimicrobial and anticancerous effects in vitro. *Journal of Photochemistry and Photobiology B: Biology*, *206*, 111841. https://doi.org/10.1016/j.jphotobiol.2020.111841

Sharmila, G., Sakthi Pradeep, R., Sandiya, K., Santhiya, S., Muthukumaran, C., Jeyanthi, J., Manoj Kumar, N., Thirumarimurugan, M. (2018). Biogenic synthesis of CuO nanoparticles using *Bauhinia tomentosa* leaves extract: Characterization and its antibacterial application. *Journal of Molecular Structure*, *1165*, 288-292. https://doi.org/10.1016/j.molstruc.2018.04.011

Siddiqui, H., Qureshi, M. S., Haque, F. Z. (2016). Valuation of copper oxide (CuO) nanoflakes for its suitability as an absorbing material in solar cells fabrication. *Optik*, *127*(8), 3713-3717. https://doi.org/10.1016/j.ijleo.2015.12.133

Singh, P., Singh, K. R., Verma, R., Prasad, P., Verma, R., Das, S. N., Singh, J., Singh, R. P. (2022). Preparation, antibacterial activity, and electrocatalytic detection of hydrazine based on biogenic CuFeO2/PANI nanocomposites synthesized using *Aloe barbadensis* Miller. *New Journal of Chemistry*, *46*(18), 8805-8816. https://doi.org/10.1039/D2NJ00913G

Sivaraj, R., Rahman, P. K. S. M., Rajiv, P., Salam, H. A., Venckatesh, R. (2014). Biogenic copper oxide nanoparticles synthesis using *Tabernaemontana divaricate* leaf extract and its antibacterial activity against urinary tract pathogen. *Spectrochimica Acta Part A: Molecular and Biomolecular Spectroscopy*, *133*, 178-181. https://doi.org/10.1016/j.saa.2014.05.048

Sougandhi, P. R. & Ramanaiah, S. (2020). Green synthesis and spectral characterization of silver nanoparticles from *Psidium guajava* leaf extract. *Inorganic and Nano-Metal Chemistry*, *50*(12), 1290-1294. https://www.tandfonline.com/doi/abs/10.1080/24701556.2020.1745839

Tamoradi, T. & Mousavi, S. M. (2020). In situ biogenic synthesis of functionalized magnetic nanoparticles with Ni complex by using a plant extract (Pistachio Leaf) and its catalytic evaluation towards polyhydroquinoline derivatives in green conditions. *Polyhedron*, *175*, 114211. https://doi.org/10.1016/j.poly.2019.114211

Veisi, H., Karmakar, B., Tamoradi, T., Tayebee, R., Sajjadifar, S., Lotfi, S., Maleki, B., Hemmati, S. (2021). Bio-inspired synthesis of palladium nanoparticles fabricated magnetic Fe3O4 nanocomposite over *Fritillaria imperialis* flower extract as an efficient recyclable catalyst for the reduction of nitroarenes. *Scientific Reports*, *11*(1), Article 1. https://doi.org/10.1038/s41598-021-83854-1

Yalcin, A. O., de Nijs, B., Fan, Z., Tichelaar, F. D., Vanmaekelbergh, D., van Blaaderen, A., Vlugt, T. J. H., van Huis, M. A., Zandbergen, H. W. (2014). Core-shell reconfiguration through thermal annealing in Fe(x)O/CoFe2O4 ordered 2D nanocrystal arrays. *Nanotechnology*, *25*(5), 055601. https://doi.org/10.1088/0957-4484/25/5/055601

Yang, Y., Aqeel Ashraf, M., Fakhri, A., Kumar Gupta, V., Zhang, D. (2021). Facile synthesis of gold-silver/copper sulfide nanoparticles for the selective/sensitive detection of chromium, photochemical and bactericidal application. *Spectrochimica Acta Part A: Molecular and Biomolecular Spectroscopy*, *249*, 119324. https://doi.org/10.1016/j.saa.2020.119324

Yoonus, J., Resmi, R., Beena, B. (2021). Evaluation of antibacterial and anticancer activity of green synthesized iron oxide (α-Fe2O3) nanoparticles. *Materials Today: Proceedings*, *46*, 2969-2974. https://doi.org/10.1016/j.matpr.2020.12.426

Zahn, D., Landers, J., Buchwald, J., Diegel, M., Salamon, S., Müller, R., Köhler, M., Ecke, G., Wende, H., Dutz, S. (2022). Ferrimagnetic Large Single Domain Iron Oxide Nanoparticles for Hyperthermia Applications. *Nanomaterials*, *12*(3), Article 3. https://doi.org/10.3390/nano12030343.